

Numerical study of parameters influence over the dynamics of a piezo-magneto-elastic energy harvesting device

Vinicius Gonçalves Lopes¹

NUMERICO - Núcleo de Modelagem e Experimentação Computacional
Universidade do Estado do Rio de Janeiro (UERJ)

João Victor Ligier Lopes Peterson²

NUMERICO - Núcleo de Modelagem e Experimentação Computacional
Universidade do Estado do Rio de Janeiro (UERJ)

Americo Cunha Jr³

NUMERICO - Núcleo de Modelagem e Experimentação Computacional
Universidade do Estado do Rio de Janeiro (UERJ)

Abstract. This work deals with the study of a piezoelectric energy harvesting device, aiming to identify parameters value that produce chaotic and non-chaotic behavior. Two different initial conditions sets are analysed. For each one, bifurcation diagrams where forcing amplitude and excitation frequency are varied, are computed and analysed, showing the existence of chaotic and regular regions.

keywords. Non-linear dynamics, energy harvesting, bi-stable system, piezo-magneto-elastic beam, bifurcation diagram, chaos.

1 Introduction

Harvesting devices are mechanisms which, due to its materials' physical-chemical properties, can collect energy from abundant external sources (heat, pressure, vibration, etc), store and convert into electrical power [6], like piezoelectric and pyroelectric ones.

Some of best applications are as alternative electrical supply for small demands, even in nano scale as described in [2–4], boarded equipment or those placed far from distribution regular systems, as exemplified by [7] for wireless sensors.

Among the most promising harvesting devices today are those with bi-stable configuration, with the possibility of occurrence of chaos [5,8]. A look over the mathematical model proposed by [5] shows incidence of chaos can be directly associated with its parameters and initial conditions, what emphasizes a well-characterization system importance.

¹vinicius.lopes@uerj.br

²joao.peterson@uerj.br

³americo@ime.uerj.br

This work concerns to study dynamic behavior of piezo-magneto-elastic energy harvesting device proposed by [5], analysing its responses for different initial conditions sets and forcing parameters, through respective bifurcation diagrams, aiming to identify regions of values where most able to provide non-chaotic outputs.

Next section brings a objective description of device's physical and mathematical models; third one presents computational approach adopted, solution strategy and respective results are presented and discussed; finally, last section gathers main contributions and conclusions of proposed study.

2 Nonlinear Dynamics Modeling

2.1 Physical model

Analysed device is depicted in Figure 1. A slim ferromagnetic cantilever beam, connected to the top of rigid structure, is exposed to magnetic field effect of two magnets, placed in the lower part of structure. An external excitation source provides vibration, exciting beam, thus piezoelectric material plates coupled in its fixed edge, which converts kinetics into electrical energy. Here, It is only considered displacement occurring in forcing oscillation direction.

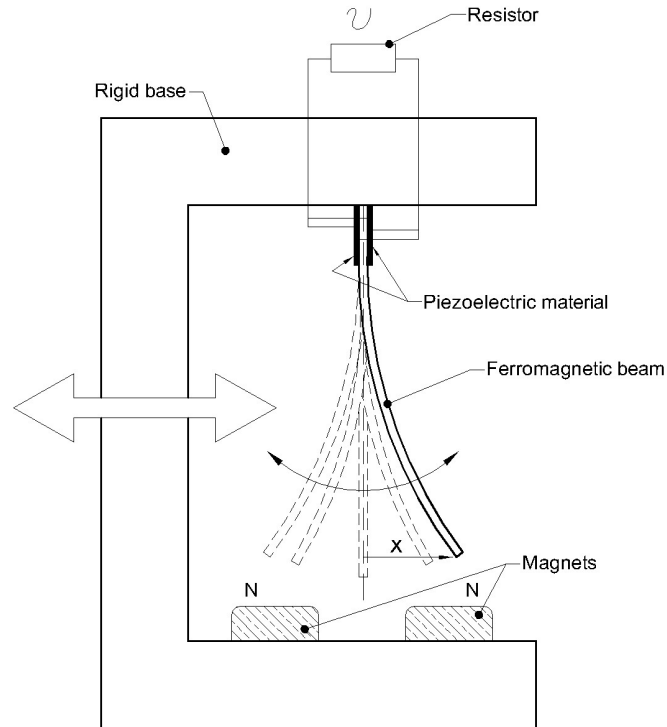


Figure 1: Schematic representation of the bi-stable energy harvesting device proposed by [5].

2.2 Mathematical model

The dynamic behavior of the energy harvesting device is described by the following system of ordinary differential equations (ODE) [5]

$$\ddot{x} + 2\xi\dot{x} - \frac{1}{2}x(1 - x^2) - \chi v = f \cos \Omega t, \quad (1)$$

$$\dot{v} + \lambda v + \kappa\dot{x} = 0, \quad (2)$$

where x represents beam's extreme displacement, ξ , the mechanical damping ratio, χ , a piezoelectric coupling term in mechanical equation, f , the amplitude of excitation, Ω , the forced excitation frequency, and v , the output voltage; in electrical circuit equation, κ means a piezoelectric coupling term and, finally, λ is a reciprocal time constant. All parameters are dimensionless, assumed initially as $\Omega = 0.8$, $\xi = 0.01$, $\chi = 0.05$, $\kappa = 0.5$ and $\lambda = 0.05$.

For problem solution, initial conditions of displacement, velocity and voltage, respectively, x_0 , \dot{x}_0 and v_0 , will be specified in next section for different analysis set.

3 Results and Discussion

In order to integrate the initial value problem of Eqs.(1) and (2), a Runge-Kutta method of fourth order is employed. To compute the first bifurcation diagram the parameter f is varied from 0.045 to 0.12, using 1200 evenly spaced points. Initial conditions are assumed as $x_0 = 1$, $\dot{x}_0 = 0$, and $v_0 = 0$; model parameters are the ones presented in section 2.2. In Figure 2 the reader can see a comparison of this diagram and a reference diagram obtained by [1]. This comparison is done in order to verify if the bifurcation diagram calculation is well done.

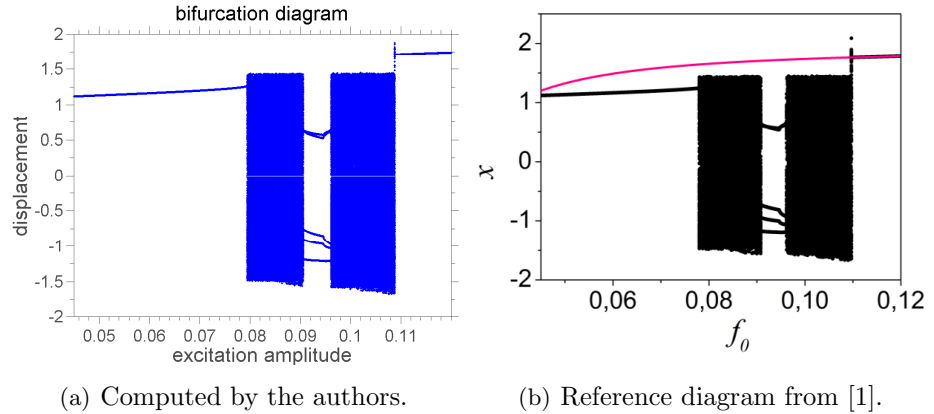


Figure 2: Bifurcation diagrams of forcing amplitude versus displacement. (a) Computed by the authors. (b) Reference diagram from [1].

Diagrams are generated for two cases for the same model parameters values from section 2.2 and different initial conditions sets, named as no initial displacement (NID), what means $x_0 = 0$, $\dot{x}_0 = 1$ and $v_0 = 1$, and no initial velocity (NIV), where $x_0 = 1$, $\dot{x}_0 = 0$ and $v_0 = 1$, for which response behavior is analysed.

In first case, different values for excitation amplitude are taken, while other parameters remain constant. Second case deals with it in the same way, but for different excitation frequency values. Diagrams observable limits are empirically defined, based in those employed by [1].

In the NID case, diagrams representing different values of forcing amplitude influence over beam extreme displacement, its velocity and output voltage are featured in Figure 3. In this case, f is taken from 0.045 to 0.12. Response does not present any chaotic pattern, what means that with these initial conditions, regular voltage is obtained for whole observable range of excitation amplitude.

A similar analysis with excitation frequency, ranging from 0.3 to 1.4, provides diagrams shown in Figure 4. Here, a blurred region appears when Ω is about 0.8, characterizing chaotic behavior. Those uniquenesses must be well known when it comes to experimentation.

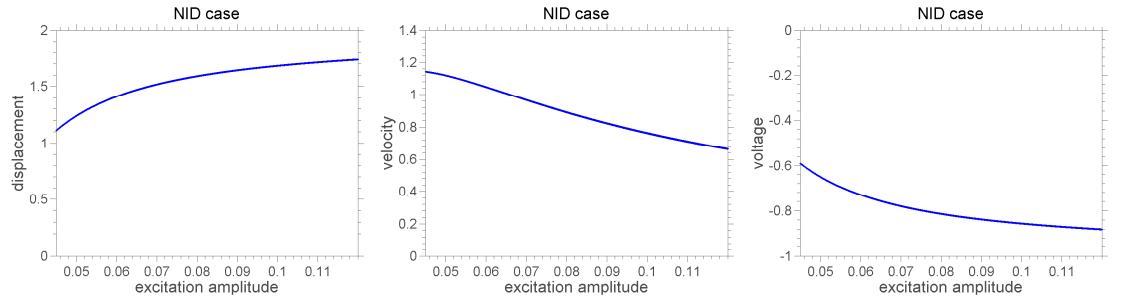


Figure 3: Bifurcation diagrams of forcing amplitude versus displacement, velocity and voltage, for $x_0 = 0$, $\dot{x}_0 = 1$, and $v_0 = 1$.

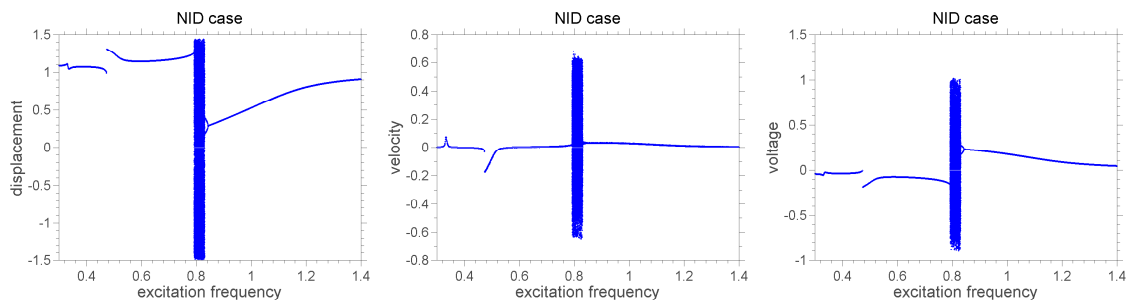


Figure 4: Bifurcation diagrams of excitation frequency versus displacement, velocity and voltage, for $x_0 = 0$, $\dot{x}_0 = 1$, and $v_0 = 1$.

In NIV case, diagrams illustrating system response for different forcing amplitude and excitation frequency are presented, respectively, in Figures 5 and 6, for the same observable intervals of NID case.

First one shows two chaotic regions when f varies from 0.08 to 0.11, with a regular zone of five periods between them. Second one exhibits regular behavior for almost all range of values, except when Ω is near of 0.8, identically to NID case.

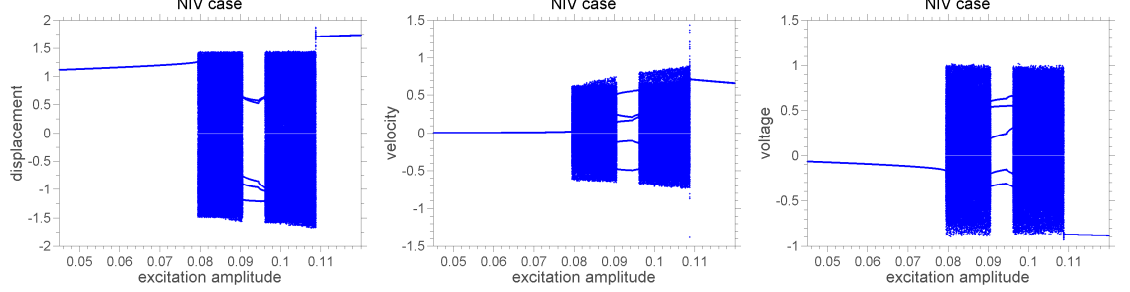


Figure 5: Bifurcation diagrams of excitation frequency versus displacement, velocity and voltage, for $x_0 = 1$, $\dot{x}_0 = 0$ and $v_0 = 1$.

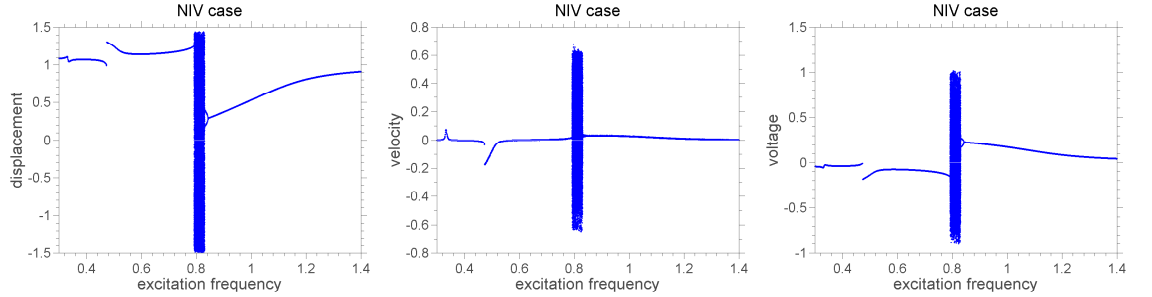


Figure 6: Bifurcation diagrams of excitation frequency versus displacement, velocity and voltage, for $x_0 = 1$, $\dot{x}_0 = 0$ and $v_0 = 1$.

4 Final Remarks

This paper analysed a harvesting device using bifurcation diagrams for two different sets of initial conditions. For each of these, different parameters values are considered, varying excitation frequency and amplitude, intending to characterize regions of regular behavior.

As its main contributions can be highlighted the obtained results about system dynamics, regarding excitation frequency and forcing amplitude effects over it, specially output voltage.

In future works, authors intent to analyse how other model parameters influence the system dynamics aiming to improve and extending device behavior characterization.

Acknowledgments

The authors are indebted to the Brazilian agencies CNPq, CAPES, and FAPERJ for the financial support given to this research.

References

- [1] T. Leite, A. S. de Paula, A. T. Fabro and M. Savi, A numerical analysis of the electrical output response of a nonlinear piezoelectric oscillator subjected to a harmonic and random excitation, *XXXVII Iberian Latin American Congress on Computational Methods in Engineering, Brasilia, DF, Brazil*.
- [2] Z. L. Wang and J. Song, Piezoelectric Nanogenerators Based on Zinc Oxide Nanowire Arrays, *Science* 312 (2006) 242-246.
- [3] A. Koka, Z. Zhou, H. Tang and H. A. Sodano, Controlled synthesis of ultra-long vertically aligned BaTiO₃ nanowire arrays for sensing and energy harvesting applications, *Nanotechnology* 25 (2014) 375603.
- [4] M. Seol, J. Choi, J. Kim, J. Ahn, D. Moon and Y. Choi, Piezoelectric nanogenerator with a nanoforest structure, *Nano Energy* 2 (2013) 1142 - 1148.
- [5] A. Erturk, J. Hoffmann, and D. J. Inman, A piezomagnetoelastic structure for broadband vibration energy harvesting, *Applied Physics Letters*, 94:254102, 2009. <http://dx.doi.org/10.1063/1.3159815>
- [6] Mohammad H Malakooti and Henry A Sodano, 2015, Piezoelectric energy harvesting through shear mode operation, *Smart Mater. Struct.* **24** 055005 <https://doi.org/10.1088/0964-1726/24/5/055005>
- [7] A.S.M. Zahid Kausar , A. W. Reza, M. U. Saleh, and H. Ramiah, Energy wireless sensor networks by energy harvesting systems: scopes, challenges and approaches, *Renewable and Sustainable Energy Reviews*, 38:973-989, 2014. <http://dx.doi.org/10.1016/j.rser.2014.07.035>
- [8] J. V. L. L. Peterson, V. G. Lopes, and A. Cunha Jr, *Maximization of the electrical power generated by a piezo-magneto-elastic energy harvesting device*, In: XXXVI Congresso Nacional de Matemtica Aplicada e Computacional (CNMAC-2016), 2016.